CHEMISTRY
A EUROPEAN JOURNAL

DOI: 10.1002/chem.201101547

Synthetic Prodiginine Obatoclax (GX15-070) and Related Analogues: Anion Binding, Transmembrane Transport, and Cytotoxicity Properties

Borja Díaz de Greñu,[a] Paulina Iglesias Hernández,[b] Margarita Espona,[b] David Quiñonero,[c] Mark E. Light,[d] Tomás Torroba,[a] Ricardo Pérez-Tomás,[b] and Roberto Quesada*[a]

Abstract: Synthetic prodiginine obatoclax shows promise as a potential anticancer drug. This compound promotes apoptosis of cancer cells, although the mechanism of action is unclear. To date, only the inhibition of BCL-2 proteins has been proposed as a mechanism of action. To gain insight into other possible modes of action, we have studied the anion-binding properties of obatoclax and related analogues in solution, in the solid state, and by means of density functional theory calculations. These compounds are well suited to interact with anions such as chloride and bicarbonate. The anion-transport properties of the compounds synthesized were assayed in model phospholipid liposomes by using a chloride-selective-electrode technique and ^{13}C NMR spectroscopy. The results demonstrated that these compounds are efficient anion exchangers that promote chloride, bicarbonate, and nitrate transport through lipid bilayers at very low concentrations. In vitro studies on small-cell lung carcinoma cell line GLC4 showed that active ionophores are able to discharge pH gradients in living cells and the cytotoxicity of these compounds correlates well with ionophoric activity.

Keywords: antitumor agents · cytotoxicity · ionophores · liposomes · supramolecular chemistry

Introduction

Recently, development of synthetic anion transporters has attracted intense interest due the potential applications of these systems in medicinal chemistry, sensing applications, and biomembrane research.[1] The control of anion transport is crucial for cell survival, therefore, molecules and synthetic transport systems that facilitate transmembrane anion transport could display biological activity. Despite this, there are only a few studies that concern the effect of anion transporters in living cells.[2] Prodigiosin stands out as the best-studied naturally occurring small-molecule anionophore (Scheme 1).[3] This alkaloid named a family of red pigments (the prodiginines), characterized by a 4-methoxy-2,2′-bipyrrolpyrromethene core, produced by several bacteria strains.[4] The physiological functions of the prodiginines in the producing organisms are not clear, nevertheless, they display a broad range of potentially useful biological activities. The antimicrobial, antimalarial, immunosuppressive, and cytotoxic activity of these compounds are well documented.[5] Multiple mechanisms/cellular targets have been related to the biological activity of prodiginines, ionophoric activity included.[6] Prodiginines can interfere with signal-transduction pathways and affect mitogen-activated protein kinases (MAPKs), facilitate double-strand DNA cleavage in the presence of Cu^{II}, induce cell-cycle arrest, and disrupt intracellular pH gradients. Recently, the prodiginines have emerged as a novel group of agents with proapoptotic anticancer properties.[7] In this regard, the synthetic prodiginine obatoclax (GX15-070, **1a**) is of singular relevance because it shows promise as an anticancer drug.[8] This compound, commercially developed by the pharmaceutical company Gemin X (recently acquired by Cephalon), has shown promising activity in both preclinical and clinical trials across multiple cancer indications and encouraging results in phase II clinical trials, in combination with carboplatin and etoposide, in front-line extensive-stage small-cell lung cancer (SCLC). A number of studies have appeared in the literature that link the proapoptotic activity of **1a** to BCL-2 inhibition (BCL-2 are a family of proteins that control the commitment to apoptotic cell death in mammals), whereas other modes of action of this compound remain largely un-

[a] B. Díaz de Greñu, Prof. T. Torroba, Dr. R. Quesada
Departamento de Química, Facultad de Ciencias
Universidad de Burgos
09001 Burgos (Spain)
Fax: (+34)-947-258-013
E-mail: rquesada@ubu.es

[b] P. I. Hernández, M. Espona, Prof. R. Pérez-Tomás
Department of Pathology and Experimental Therapeutics
Universidad de Barcelona, Barcelona (Spain)

[c] Dr. D. Quiñonero
Departament de Quimica
Universitat de les Illes Balears
07122 Palma de Mallorca (Spain)

[d] Dr. M. E. Light
School of Chemistry
University of Southampton
SO17 1BJ, Southampton (UK)

Supporting information for this article is available on the WWW under http://dx.doi.org/10.1002/chem.201101547.

WILEY ONLINE LIBRARY

© 2011 Wiley-VCH Verlag GmbH & Co. KGaA, Weinheim

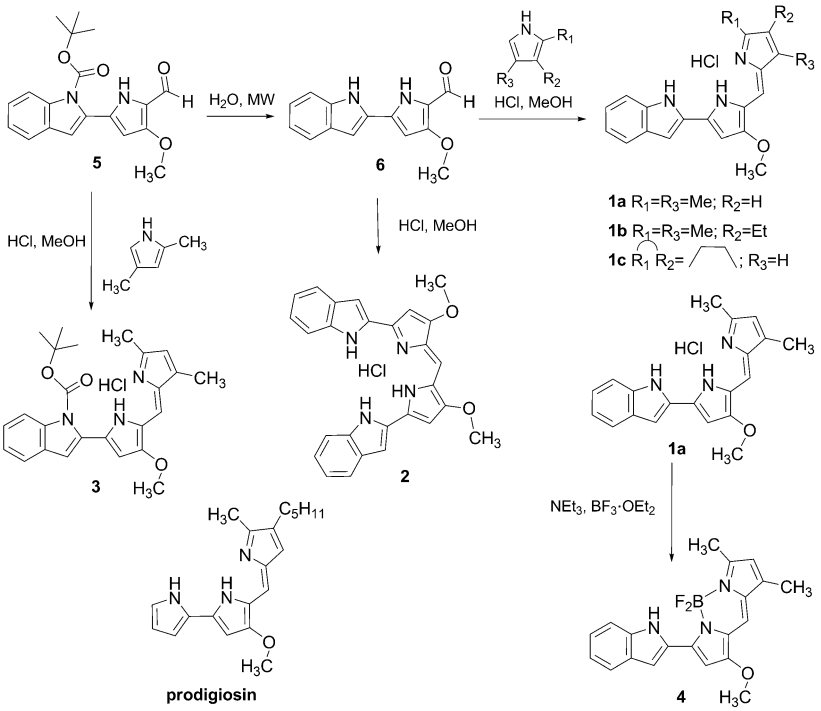

Scheme 1. Synthesis of compounds **1**–**4** (MW = microwave irradiation).

explored.[9] In this regard, it is essential to gain insight into the mode of action of these compounds to develop derivatives with improved pharmacological properties. In this work, we set out to study the anion-binding and transport properties of **1a** and related analogues, and to explore the implications of these activities on the cytotoxicity exhibited by these compounds.

Results and Discussion

Synthesis and anion-binding studies: Compounds **1a**–**c** were synthesized by using variations on reported procedures (Scheme 1).[10] Briefly, acid-catalyzed condensation of indole–pyrrole aldehyde **6** with assorted pyrroles gave **1a** and analogues **1b** and **1c** in good yields. Small amounts of a symmetrical derivative **2** were also detected in the reaction mixtures. Prompted by this result, we investigated the treatment of aldehyde **6** under acidic conditions and observed formation of the tetraheterocyclic derivative **2** in good yield. Presumably, under these conditions, partial deformylation then condensation occurred, which led to the formation of the symmetrical coupling derivative **2**. It should be noted that the analogous dipyrrolyldipyrromethene derived from prodiginine precursors has been described in bacterial extracts.[11] To evaluate the impact of the anion coordination and transport properties of the obatoclax analogues in the biological activity of these compounds we decided to prepare two new derivatives by the introduction of modifications on the NH groups. We reasoned that such variations could impact the anion binding and transport properties of these compounds, yet retain structural similarity with **1a**. First, the *N*-Boc-protected (Boc = *tert*-butoxycarbonyl) derivative **3** was synthesized from *N*-Boc-protected aldehyde **5**. Compound **3** represents an obatoclax analogue with the NH group of the indole ring unavailable for anion coordination. Finally, boron-dipyrromethene (BODIPY) derivative **4** was prepared from **1a**. Compound **4** is a neutral derivative with no protonable groups. In this case, the dipyrromethene unit is not available for anion binding.

The first evidence of the ability of these compounds to interact with anions came from structural studies. Solid-state structures of **1a** (as the mesylate and chloride salts), **3**·HCl, and **4** were determined by single-crystal X-ray diffraction (Figure 1).

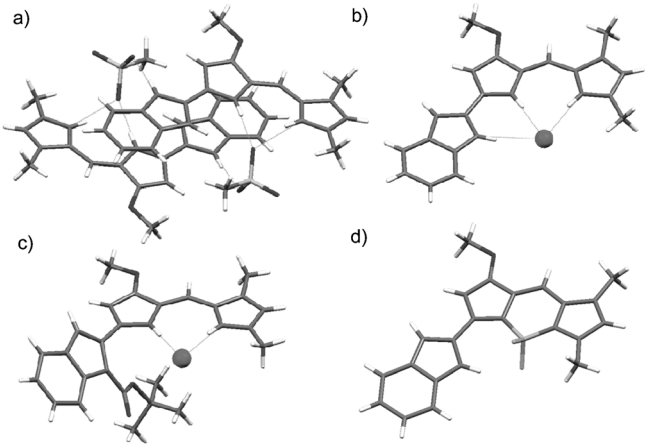

Figure 1. Representations of solid-state structures. a) **1a**·$MeSO_3H$, b) **1a**·HCl, c) **3**·HCl, d) **4**.

In the solid state, compound **1a**·$MeSO_3H$ forms 2:2 stacked dimers (Figure 1a). Each mesylate anion is coordinated to two molecules of **1a** through hydrogen bonds. One of the oxygen atoms was found to interact with the two NH groups of the dipyrromethene unit and other was coordinated to the indole NH group of the second molecule of **1a** (N–H···O distances = 2.86–2.94 Å). The tris-heterocyclic skeleton of **1a** is essentially flat and adopts a β conformation (the two pyrrole rings are in a relative *cis* disposition around the methine linkage) with the indole ring rotated

 © 2011 Wiley-VCH Verlag GmbH & Co. KGaA, Weinheim

180°. The distance between the planes that contain the two receptors is 3.37 Å. The solid-state structure of **1a**·HCl (Figure 1b) consisted of 1:1 complexes. The tris-heterocyclic skeleton of **1a** is, again, essentially flat and adopts a β conformation, with the three NH groups oriented in the same direction and engaged in hydrogen bonds with the chloride anion (N–H···Cl distances = 3.17–3.18 Å). In compound **3**·HCl the chloride anion was also found to interact with the dipyrromethene unit through hydrogen bonds (N–H···Cl distances = 3.11–3.12 Å). The presence of the *N*-Boc group forces the indole group out of the plane defined by the dipyrromethene unit with a torsion angle of 41.7°. In the solid state, compound **4** also showed an essentially flat indolyldipyrromethene core with the indole group facing the boraindacene moiety.

We next studied the anion-binding properties of **1a** in solution, as a model compound. For biological studies, **1a** is generally employed as the mesylate salt. We studied the lability of this anion and the first indication came from extraction experiments. Treatment of a solution of **1a**·$MeSO_3H$ in CH_2Cl_2 with a dilute aqueous solution of HCl resulted in formation of **1a**·HCl, whereas treatment of a solution of **1a**·HCl in CH_2Cl_2 with a dilute aqueous solution of methanesulfonic acid resulted in no change, even after several treatments. A titration experiment, monitored by ^{1}H NMR spectroscopy, of **1a**·$MeSO_3H$ with tetra-*n*-butylammonium chloride (TBACl) in $CDCl_3$ revealed that the mesylate anion is readily displaced by chloride. Upon addition of TBACl the NH signals became broader and drifted downfield, with little change noticeable beyond the addition of 1 equiv of TBACl (Figure 2). The spectrum is virtually equivalent to that of **1a**·HCl. From these data, an apparent stability constant of 6140 M^{-1} was determined by using the EQNMR computer program.[12] All of these results suggest that the mesylate anion is likely displaced in biological environments. Treatment of protonated **1a**, either as the chloride or mesylate salt, with tetraethylammonium bicarbonate ($TEAHCO_3$) in $CDCl_3$ resulted in severe broadening of the peaks in the ^{1}H NMR spectrum, which precluded the calculation of an apparent stability constant. Moreover, formation of the neutral derivative **1a** by deprotonation of the compound was also observed. In the neutral form, **1a** can also interact with anions. Titration experiments of **1a** with TBACl and $TEAHCO_3$ in CD_3CN allowed the determination of stability constants of 42 and 96 M^{-1} for chloride and bicarbonate, respectively. The affinity of **1a** for chloride is greatly reduced compared with the protonated form **1a**H^+, which reflects the lack of attractive electrostatic interaction in the neutral receptor and the more competitive nature of the solvent used.

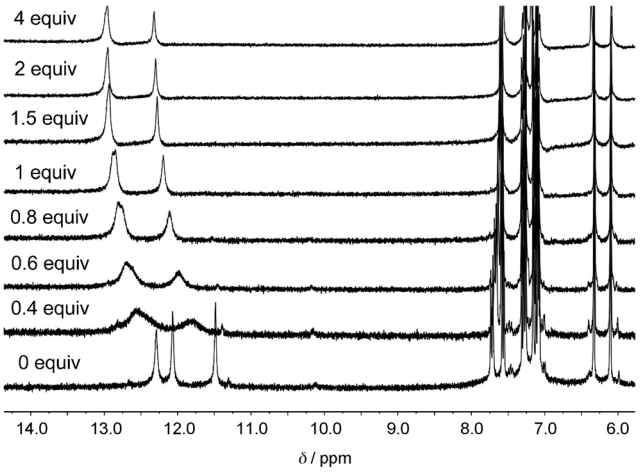

Figure 2. ^{1}H NMR spectra of **1a**·$MeSO_3H$ in $CDCl_3$ (downfield region) upon addition of increasing amounts of TBACl.

Further energetic and optimized geometric characteristics of the complexes were obtained by density functional theory (DFT) calculations (BP86/def2-QZVP). The binding energies were obtained by considering compound **1a** in its β conformation as our reference molecule. Therefore, all computed binding energies of complexes of **1a** with bicarbonate and chloride anions refer to its β conformation.[3] Likewise, the binding energies of complexes of **1a**H^+ with mesylate, bicarbonate, and chloride anions were computed by reference to **1a**H^+ in its lowest-energy conformation, in accordance with Cole's DFT calculations on prodiginines.[13] In other words, the conformation with the indole and terminal pyrrole rings rotated 180° relative to the central pyrrole ring (we dubbed this the γ conformation). At this time, we do not want to report a detailed conformational study of the receptors because the aim of this work is to study the formation of the complexes, regardless what the lowest-energy conformation of **1a** and **1a**H^+ is. To our knowledge, these are the first theoretical calculations reported for complexes of prodiginines with anions.

We have systematically explored the formation of complexes of **1a** and **1a**H^+ by consideration of different tautomers and conformers of the receptors that interact with the anions. We have computed four complexes of **1a**H^+ (see the Supporting Information, Figure S17) and nine complexes of **1a** for every anion (see the Supporting Information, Figures S18 and S19). The largest interaction energies of these complexes are collected and presented in Table 1. First, we will analyze the complexes of **1a**H^+ (Table 1, entries 1–3). It can be observed that the interaction energy of complex **1a**·HCl (Table 1, entry 2) is larger than that of complex **1a**·$MeSO_3H$ (Table 1, entry 1), both in the gas phase and in

Table 1. Interaction energies in the gas phase (ΔE) and in aqueous solution (ΔE_{solv}) for several complexes of **1a** at the RI-BP86/def2-QZVP level of theory and stability constants (K_a) at 298 K with TBACl and $TEAHCO_3$ as the anion sources.

Entry	Compound	ΔE [kcal mol^{-1}]	ΔE_{solv} [kcal mol^{-1}]	K_a [M^{-1}]
1	**1a**·$MeSO_3H$	−102.2	−5.4	–
2	**1a**·HCl	−113.1	−7.3	6140[a]
3	**1a**·H_2CO_3	−113.3	−10.7	–
4	**1a**·Cl^-	−27.5	+0.7 (−0.7)[b]	42[b]
5	**1a**·HCO_3^-	−26.9	−4.0 (−4.9)[b]	96[b]

[a] $CDCl_3$ as the solvent. [b] CH_3CN as the solvent; see text for details.

© 2011 Wiley-VCH Verlag GmbH & Co. KGaA, Weinheim

water, in agreement with our titration experiment between **1a**·$MeSO_3H$ and TBACl (Figure 2), in which $MeSO_3^-$ was displaced by Cl^-. Both in the gas phase and aqueous solution, the β isomer is the most favored conformation for anion binding, with all three N–H bonds pointing at the anion (see Figure 3). This result is also in agreement with

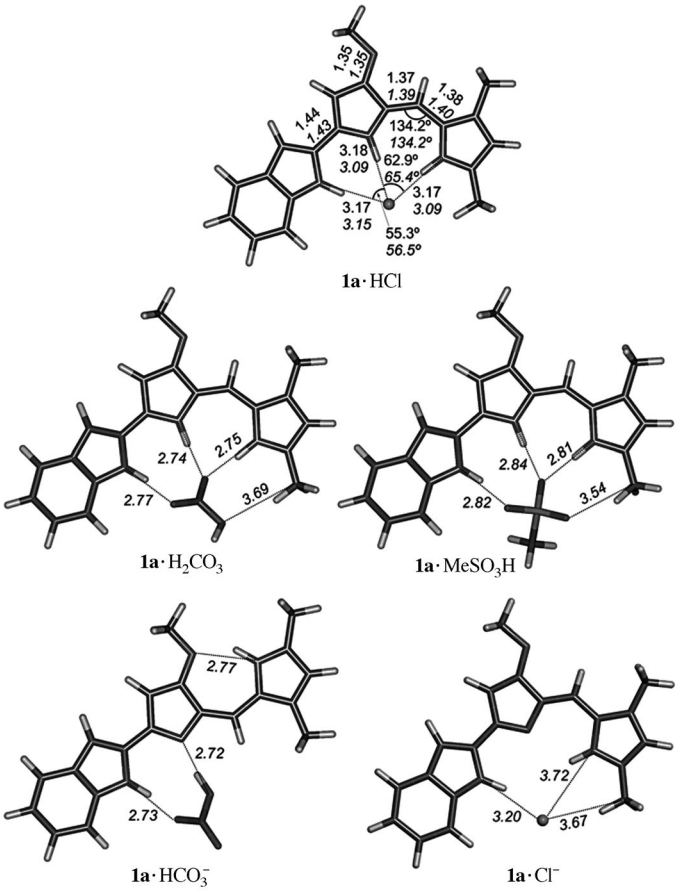

Figure 3. Top: Comparison of the **1a**·HCl optimized gas-phase geometry (italics) with the X-ray structure (plain). Rest: Optimized geometries of **1a** complexes with the largest interaction energies in water. Distances [Å], angles [°].

the correlations observed in the NOESY spectra of **1a**·HCl and **1a**·$MeSO_3H$ in CD_3Cl (see the Supporting Information, Figures S5 and S6). The order of calculated interaction energies of protonated **1a** with anions was found to be $HCO_3^- > Cl^- > MeSO_3^-$. Notably, proton abstraction to yield carbonic acid is not observed in solution for any of the calculated structures. A comparison of the optimized and experimental structures of complex **1a**·HCl supported the reliability of the theoretical level used in the analysis. In Figure 3 (top), we represent selected geometric features of the DFT solvent-free optimized complex **1a**·HCl and its crystal structure. From inspection of the results, first, we observe that both the bond lengths and angles in the optimized and experimental structures of **1a**·HCl are in excellent agreement. Second, the computed noncovalent distances between the chloride anion and the receptor are marginally shorter than the experimental values. This result is unsurprising because, in general, the equilibrium distances of complexes are shorter in the gas phase than in the solid state due to packing forces. Particularly, the chloride anion participates in an additional noncovalent interaction with a hydrogen atom (2.521 Å) of a neighboring CH_2Cl_2 solvent molecule. We have chosen complex **1a**·HCl for comparison purposes rather than **1a**·$MeSO_3H$ because the latter forms 2:2 stacked dimers in the solid state, which gives rise to a different geometrical array relative to the computed 1:1 structure (see Figures 1–3).

We also analyzed the complexes of **1a** with chloride and bicarbonate (Table 1, entries 4 and 5) and found the interaction energy for Cl^- is slightly larger than that for HCO_3^-. However, when water effects are taken into account the opposite is observed; in other words, the HCO_3^- complex is much lower in energy ($-4.0\ kcal\,mol^{-1}$) than the Cl^- analogue. In fact, the interaction energy of **1a**·Cl^- is slightly positive ($+0.7\ kcal\,mol^{-1}$), which means that the formation of **1a**·Cl^- complex is not favored in water. Nevertheless, because our experimental apparent-stability constants are measured in CD_3CN, we also carried out calculations for our complexes solvated in CH_3CN (Table 1, entries 4 and 5) for direct comparison with the experimental results. In this solvent, the interaction energies of complexes **1a**·Cl^- and **1a**·HCO_3^- are both favorable (-0.7 and $-4.9\ kcal\,mol^{-1}$, respectively) and in good agreement with the experimental stability constants (42 and $96\ M^{-1}$, respectively). In aqueous solution, the so-called α isomer (with the terminal pyrrole ring rotated 180° relative to both the indole and central pyrrole fragments, see Figure 3 and the Supporting Information, Figure S18) is the most favored conformation for the **1a**·HCO_3^- complex ($-4.0\ kcal\,mol^{-1}$) by only $0.2\ kcal\,mol^{-1}$ relative to its β counterpart, which leads to the assumption that both complexes are isoenergetic (in the gas phase the energy difference is approximately $10\ kcal\,mol^{-1}$ in favor of the β conformer). The fact that **1a**·HCO_3^- easily adopts the α conformation in water is most likely due to the formation of the intramolecular MeO···H–N hydrogen bond between the two pyrrole rings, which is stabilized by the polar aqueous media. Interestingly, formation of carbonic acid by proton abstraction is, again, not observed in aqueous solution.

Anion-transport studies: The anion-transport properties of **1**–**4** were assayed in 1-palmitoyl-2-oleoyl-*sn*-glycero-3-phosphocholine (POPC) vesicles by using a chloride-selective electrode in accordance with previously reported procedures.[14] Briefly, liposomes loaded with NaCl were suspended in an isotonic, chloride-free external medium. Chloride release promoted by **1**–**4** was monitored over time and at the end of the experiment the vesicles were lysed by the addition of detergent; the final electrode reading was used as 100% release of chloride. When the chloride-loaded vesicles were suspended in an external $NaNO_3$ solution almost quantitative chloride efflux was promoted by compounds **1a**–**c** at

 © 2011 Wiley-VCH Verlag GmbH & Co. KGaA, Weinheim

very low concentrations (25 nM, 0.005 mol% carrier/lipid concentration, added as a solution in DMSO, see Figure 4). Under these conditions, lower activity was observed for **2** (less than 60% chloride efflux after 300 s) and **3** (less than 20% chloride efflux after 300 s). Compound **4** promoted no

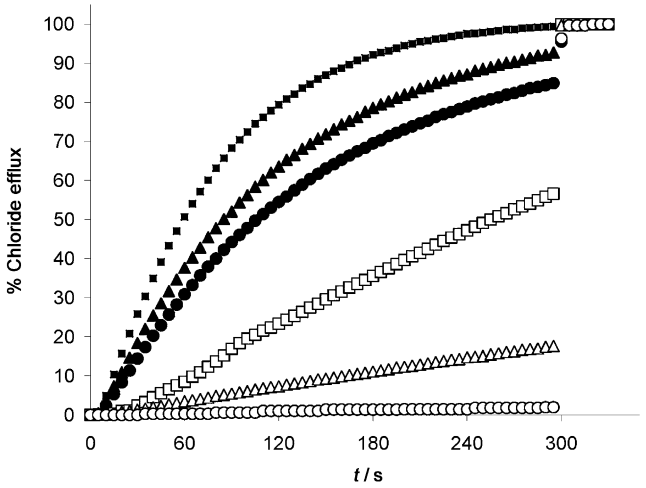

Figure 4. Chloride efflux promoted by **1**–**4** (25 nM, 0.005 mol% carrier/lipid concentration) in unilamellar POPC vesicles. Vesicles loaded with NaCl (476 mM) buffered at pH 7.2 dispersed in $NaNO_3$ (476 mM) buffered at pH 7.2 with phosphate (10 mM). Each trace represents the average of three trials. (▲**1a**, ■**1b**, ●**1c**, □**2**, △**3**, ○**4**).

significant chloride efflux. When the vesicles were suspended in an external medium composed of sodium sulfate, addition of **1**–**4** resulted in a very limited chloride efflux. Addition of an external pulse of $NaHCO_3$ in these assays resulted in a switch-on of the chloride release. The results obtained for carrier loadings of 250 nM (0.05 mol% carrier/lipid concentration, added as a solution in DMSO) are shown in Figure 5. Compound **1b** was the most active in this assay, whereas compound **4** promoted no significant chloride efflux. Because chloride and bicarbonate are the most abundant anions in physiological fluids, this result is more significant for biological applications. Hill analyses were performed for the chloride efflux observed under these conditions and the EC_{50} values (concentration needed to obtain 50% of chloride release after 290 s) are summarized in Table 2 (see the Supporting Information, Figures S23–S27 for details).[15] The results observed in the liposome assays are consistent with a dominant anion-exchange mechanism for the facilitated chloride efflux from the liposomes under these conditions. The nature of the external anion impacted dramatically the rate of chloride efflux promoted by these compounds. The relatively higher hydrophilicity of bicarbonate compared with nitrate resulted in lower chloride efflux at higher carrier loadings. In both cases the observed activity order is **1b** > **1a** > **1c** > **2** > **3** ≫ **4**.

Direct evidence of bicarbonate transport mediated by these compounds was obtained from ^{13}C NMR spectroscopy experiments (see Figure 6 and the Supporting Information).[16] First, POPC liposomes filled with $NaH^{13}CO_3$ were

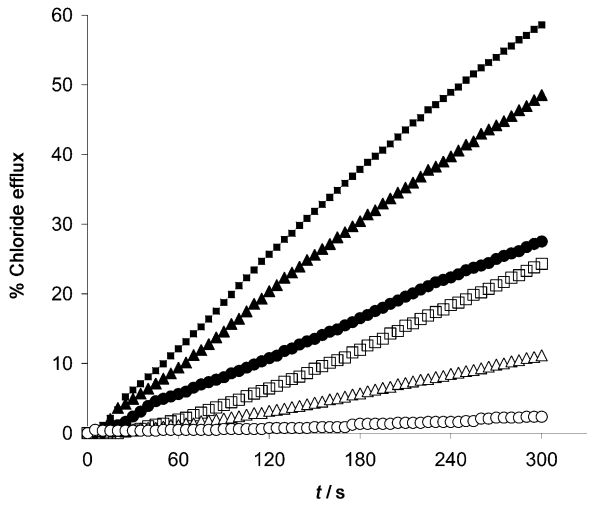

Figure 5. Chloride efflux promoted by **1**–**4** (250 nM, 0.05 mol% carrier/lipid concentration) in unilamellar POPC vesicles. Vesicles loaded with NaCl (451 mM) buffered at pH 7.2 with phosphate (20 mM) dispersed in Na_2SO_4 (150 mM) buffered at pH 7.2 upon addition of a $NaHCO_3$ pulse to make the extravesicular bicarbonate concentration 40 mM. Each trace represents the average of three trials. (▲**1a**, ■**1b**, ●**1c**, □**2**, △**3**, ○**4**).

Table 2. IC_{50} values of compounds **1**–**3** obtained from MTT assay on the GLC4 cell line at 24, 48, and 72 h exposure time. Results depicted represent a mean of three independent experiments with standard deviation. EC_{50} values (concentration needed to achieve 50% of chloride efflux after 290 s) of compounds **1**–**3** for the bicarbonate antiport process.

Compound	IC_{50} [μM]			EC_{50} [μM]
	24 h	48 h	72 h	
1a	1.61 ± 0.15	0.25 ± 0.54	0.13 ± 0.10	0.28 ± 0.01
1b	1.02 ± 0.21	0.29 ± 0.07	0.23 ± 0.06	0.18 ± 0.02
1c	0.96 ± 0.05	0.42 ± 0.19	0.32 ± 0.02	0.75 ± 0.04
2	0.97 ± 0.12	0.60 ± 0.05	0.61 ± 0.13	2.10 ± 0.25
3	–	2.01 ± 1.08	1.68 ± 0.11	18.90 ± 3.13

suspended in a solution of Na_2SO_4 in water. Two ^{13}C NMR signals that corresponded to intravesicular and extravesicular $H^{13}CO_3^-$ could be observed (Figure 6a). Bicarbonate efflux from the interior of the vesicles occurred after addition of an external pulse of NaCl, and a DMSO solution of the carrier in the case of active anionophore **1b**. This event is reflected by the disappearance of the broad signal that corresponds to encapsulated $H^{13}CO_3^-$, with only a sharp signal for extravesicular $H^{13}CO_3^-$ appearing in the ^{13}C NMR spectrum (Figure 6b, left). Little change in the ^{13}C NMR spectrum was observed when inactive carrier molecule **4** was added (Figure 6b, right). Addition of paramagnetic Mn^{2+} resulted in broadening of the extravesicular $H^{13}CO_3^-$ signal, whereas the encapsulated bicarbonate signal was not affected because Mn^{2+} cannot cross the lipid bilayer. Thus, only the sharp signal is erased in the case of vesicles treated with **4** (Figure 6c, right) and the broad signal for the encapsulated $H^{13}CO_3^-$ remained clearly visible. In the case of **1b** (Figure 6c, left) the signal is broadened to the baseline. The

 © 2011 Wiley-VCH Verlag GmbH & Co. KGaA, Weinheim

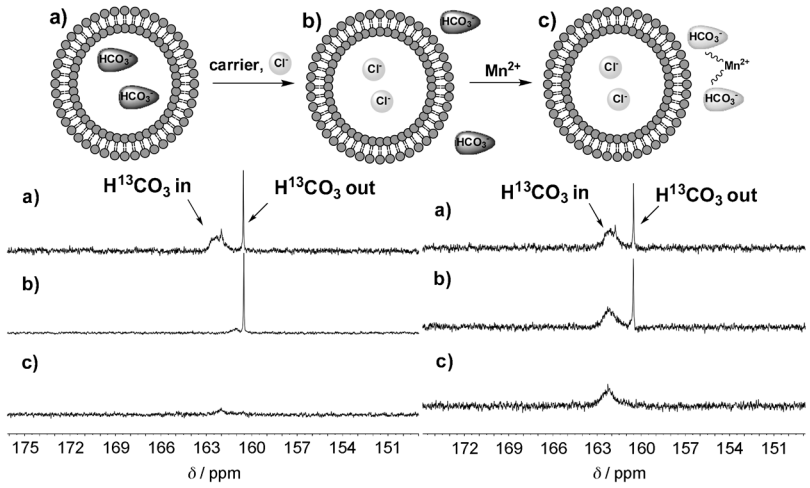

Figure 6. ^{13}C NMR spectra evidencing the facilitated bicarbonate/chloride exchange. a) POPC vesicles loaded with $NaH^{13}CO_3$ (500 mM) dispersed in Na_2SO_4 (162 mM) buffered at pH 7.2 with phosphate (20 mM). b) After addition of NaCl (50 mM) and **1b** (left) or **4** (right) (119 μM, 0.16 mol% carrier/lipid concentration). c) After addition of $MnCl_2$ (0.5 mM), a paramagnetic reagent affecting only extravesicular $H^{13}CO_3^-$ anions.

assay described for compound **4** also served as a control experiment for the leakage of bicarbonate upon addition of a chloride pulse or for unspecific detergent effects. Similar results to those described in the case of **1b** were observed for **1a**, whereas addition of **3** resulted in moderate bicarbonate efflux under the same conditions, which reflected the poorer anion exchange activity displayed by this compound.

The anion-transport assays revealed that compounds **1a–c** are able to function as efficient anion carriers. Varying the number of hydrogen-bond donors, as in **2** and **3**, resulted in diminished transport activity. Compound **4** did not function as anion carrier.

In vitro studies: The in vitro ionophoric activity of compounds **1–4** on SCLC cell line GLC4 was studied by vital staining with acridine orange (AO). This cell-permeable dye accumulates in acidic compartments such as lysosomes and exhibits a characteristic orange fluorescence emission as a result of its protonation, or green fluorescence at higher pH.[17] When GLC4 cells were stained with AO, granular orange fluorescence was observed in the cytoplasm (Figure 7a), suggestive of acidified lysosomes. The cells were treated with compounds **1–4** (800 nM concentrations) for 1 h and representative results are shown in Figure 7. Cells treated with compounds **1a** and **3** showed a complete disappearance of the orange emission (Figure 7b and c). Similar results were obtained with **1b**, **1c**, and **2**. On the other hand, cells treated with **4** showed no changes (Figure 7d). These results correlate well with the activity observed in the liposome assays. Only active anionophores induce an increase in the lysosomal pH, whereas the inactive carrier **4** did not affect intracellular pH. Based on the results obtained in the liposome assays, facilitated influx of bicarbonate to the interior of the lysosomes could be proposed as the mechanism responsible for the increase of the internal pH, although other mechanisms cannot be ruled out.

The in vitro cytotoxic activity of compounds **1–4** was tested on the GLC4 cell line. We used this cell line as a model due to the proven usefulness of **1a** in the treatment of this condition. Dose–response curves for compounds **1–4** in the 72 h viability assay in GLC4 cells are shown in Figure 8. IC_{50} values obtained from 24, 48, and 72 h viability assays are presented in Table 2. Hoechst staining revealed apoptosis as the cell-death mechanism, in agreement with the reported activity of these derivatives (see the Supporting Information). In the 72 h assay, the most active compound was **1a** with an IC_{50} value of 0.13 ± 0.10 μM. Compound **3** displayed a significantly reduced toxicity relative to **1a–c**, with an IC_{50} value of 1.68 ± 0.11 μM at 72 h, and compound **4** is a non-cytotoxic derivative. These results correlate well with the activity as anion exchangers studied in liposomes (Table 2, EC_{50} values). The most active anionophores **1a–c** are the most potent derivatives, whereas cytotoxicity diminished in the case of **2** and **3**, as did activity

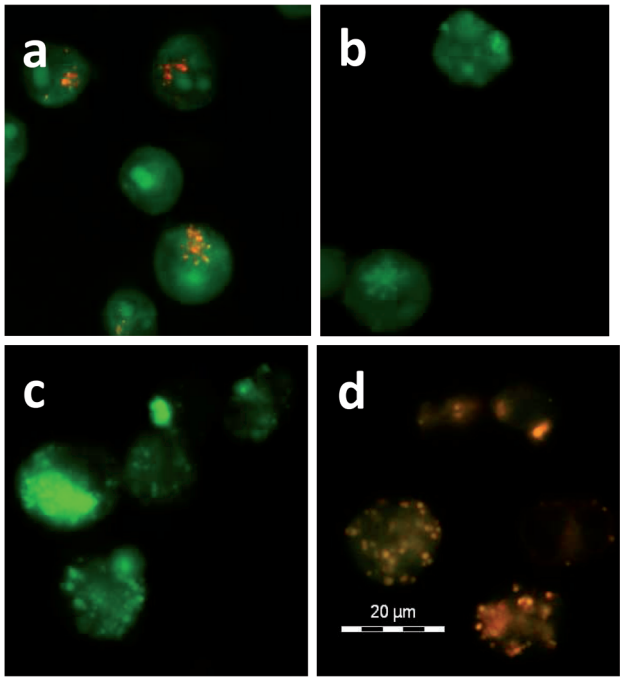

Figure 7. AO staining of the GLC4 cell line after 1 h exposure to the indicate compounds at 800 nM concentration. a) Untreated cells (control). b) Cells treated with **1a**. c) Cells treated with **3**. d) Cells treated with **4**. a),d) Cells showed granular orange fluorescence in the cytoplasm. b),c) Cells showed complete disappearance of orange fluorescence on the cytoplasm granules

 © 2011 Wiley-VCH Verlag GmbH & Co. KGaA, Weinheim

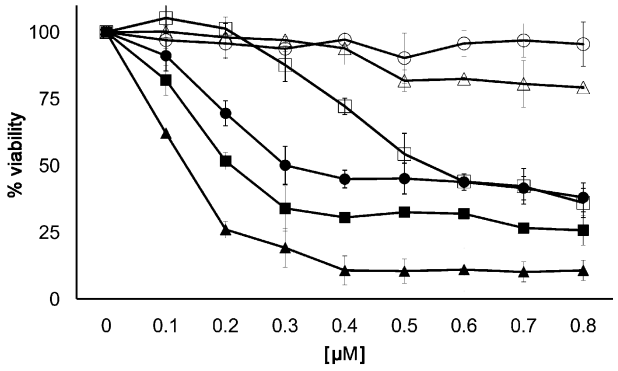

Figure 8. Dose–response curves for compounds **1**–**4** on the viability of GLC4 cell line. The results are the mean ± SEM for three independent experiments and are expressed as % viability compared with control. Error bars represent the standard deviation. (▲**1a**, ■**1b**, ●**1c**, □**2**, △**3**, ○**4**).

in the anion-transport assays. Compound **4** was found to be inactive in these assays and displayed no cytotoxicity. The compounds studied showed no marked toxicity on nonmalignant HaCaT cells at IC_{50} concentrations.

Conclusion

In this study we have investigated the anion-binding properties of obatoclax (**1a**) by using DFT calculations, as well as solution and structural studies. This compound is well suited to interact with anions through hydrogen bonds and preferentially adopts a β conformation. Compound **1a** and related analogues **1b** and **1c** are highly active anionophores capable of promoting chloride and bicarbonate (and nitrate) transport in model phospholipid liposomes. Manipulation of these compounds by variation of the number of hydrogen-bond donors resulted in diminished anion-carrier ability. The anionophoric activity correlated well with the results observed in the in vitro studies. Active anion carriers are able to discharge pH gradients in living cells and the most active anionophores were found to be the most potent cytotoxic derivatives. Inactive, yet structurally very related molecules (such as compound **4**), did not show cytotoxicity against the GLC4 cell line. These findings led us to suggest that anion transport plays a relevant role in the mechanism of action of these compounds. Thus, development of new derivatives with improved anion-transport abilities could lead to new drugs with improved pharmacological properties. In this regard, the straightforward liposome assays could be useful for the screening of new candidates. Efforts in these directions are currently underway in our laboratories.

Experimental Section

General procedures and methods: Commercial reagents were used as received without any further purification. NMR spectra were recorded on Varian Mercury 300 MHz and Varian Unity Inova 400 MHz spectrometers. Chemical shifts (δ) are reported in ppm, referenced to the residual solvent peak; coupling constants (J) are reported in Hz. HRMS were recorded on a Micromass Autospec S-2 spectrometer by using the electrospray ionization technique at 70 eV. Microwave reactions were performed in a Biotage Initiator 2.0 microwave. Compound **5** was prepared as described.[10]

Compound 6: Compound **5** (0.15 g, 0.44 mmol) was suspended in water (18 mL). The mixture was heated at 170 °C for 35 min under MW irradiation. Once cold, the solid was filtered off and washed with water to afford **6** (0.096 g, 91 %) as a greenish powder. ^{1}H NMR (300 MHz, [D$_6$]DMSO): δ = 11.86 (s, 1H; NH), 11.46 (s, 1H; NH), 9.42 (s, 1H; CHO), 7.53 (d, J = 6.9 Hz, 1H; ArH), 7.39 (d, J = 6.9 Hz, 1H; ArH), 7.13 (t, J = 6.9 Hz, 1H), 7.11 (s, 1H), 7.01 (t, J = 6.9 Hz, 1H; ArH), 6.55 (s, 1H), 3.88 ppm (s, 3H; OCH_3); ^{13}C NMR (75 MHz, [D$_6$]DMSO): δ = 173.12, 158.14, 136.80, 131.84, 129.47, 128.12 (CH), 122.44 (CH), 120.44 (CH), 119.79 (CH), 118.63 (CH), 111.31 (CH), 100.69, 93.28, 57.97 ppm (CH_3).

Compound 1a·HCl: Under an inert atmosphere, **6** (0.1 g, 0.42 mmol) was dissolved in methanol (5 mL), then 2,4-dimethylpyrrole (86 μL, 0.83 mmol) was added, followed by dropwise addition of a solution of HCl in methanol (1.25 M, 0.66 mL). The color changed to dark purple and the mixture was stirred overnight. The solid formed was filtered off and washed with cold methanol (1 mL) to afford **1a**·HCl (0.137 g, 93 %) as a dark-purple crystalline solid. ^{1}H NMR (300 MHz, $CDCl_3$): δ = 12.89 (s, 1H; NH), 12.82 (s, 1H; NH), 12.26 (s, 1H; NH), 7.57 (d, J = 7.2 Hz, 1H; ArH), 7.53 (d, J = 7.2 Hz, 1H; ArH), 7.29 (t, J = 7.2 Hz, 1H; ArH), 7.08 (t, J = 7.2 Hz, 1H; ArH), 7.07 (s, 1H), 6.98 (s, 1H), 6.24 (s, 1H), 6.05 (s, 1H), 3.97 (s, 3H; OCH_3), 2.60 (s, 3H; CH_3), 2.28 ppm (s, 3H; CH_3); ^{13}C NMR (75 MHz, $CDCl_3$): δ = 164.89, 150.39, 146.21, 142.50, 138.80, 127.81, 127.03, 125.54, 125.41 (CH), 121.31 (CH), 120.69 (CH), 119.72, 115.67 (CH), 114.67 (CH), 112.50 (CH), 108.77 (CH), 94.01 (CH), 58.64 (OCH_3), 14.10 (CH_3), 11.96 ppm (CH_3); HRMS (EI): m/z calcd for $C_{19}H_{20}N_3O$: 317.15; found: 317.15.

Compound 1a·MeSO$_3$H: Compound **1a**·$MeSO_3H$ was obtained as described for **1a**·HCl by using methanesulfonic acid as a catalyst to afford **1a**·$MeSO_3H$ (0.142 g, 82 %) as a dark-purple crystalline solid. ^{1}H NMR (300 MHz, $CDCl_3$): δ = 12.23 (s, 1H; NH), 11.98 (s, 1H; NH), 11.43 (s, 1H; NH), 7.69 (d, J = 8.3 Hz, 1H; ArH), 7.52 (d, J = 8.0 Hz, 1H; ArH), 7.26 (t, J = 5.7 Hz, 1H; ArH), 7.13 (s, 1H), 7.05 (t, J = 7.2 Hz, 1H; ArH), 7.01 (s, 1H), 6.31 (d, J = 1.9 Hz, 1H), 6.08 (s, 1H), 4.01 (s, 3H; OCH_3), 2.97 (s, 3H; SCH_3), 2.62 (s, 3H; CH_3), 2.29 ppm (s, 3H, CH_3).

Compound 1a: Compound **1a**·HCl (0.040 g, 0.11 mmol) was dissolved in CH_2Cl_2 (20 mL). The solution was treated with a 1 % aqueous solution of NaOH (30 mL) and the color changed from deep red to orange. The organic phase was dried over anhydrous Na_2SO_4 and the solvent was removed under reduced pressure. Compound **1a** (0.035 g, 98 %) was obtained as an orange solid. ^{1}H NMR (300 MHz, $CDCl_3$): δ = 12.05 (s, 1H; NH), 7.49 (d, J = 8.1 Hz, 1H; ArH), 7.11 (s, 1H), 7.02 (t, J = 8.1 Hz, 1H; ArH), 6.93 (t, J = 8.1 Hz, 1H; ArH), 6.90 (s, 1H), 6.77 (d, J = 8.1 Hz, 1H; ArH), 6.34 (s, 1H), 5.67 (s, 1H), 4.08 (s, 3H; OCH_3), 2.17 (s, 3H; CH_3), 1.78 ppm (s, 3H; CH_3); ^{13}C NMR (75 MHz, $CDCl_3$): δ = 168.87, 158.55, 140.97, 137.75, 136.30, 133.98, 133.82, 128.43, 126.71, 123.31 (CH), 120.76 (CH), 119.52 (CH), 115.67 (CH), 112.61 (CH), 111.49 (CH), 104.68 (CH), 96.01 (CH), 58.57 (OCH_3), 12.15 (CH_3), 11.44 ppm (CH_3); HRMS (EI): m/z calcd for $C_{19}H_{20}N_3O$: 317.1528; found: 317.1539.

Compound 1b·HCl: Compound **1b**·HCl was prepared as described for **1a**·HCl, from **6** (0.1 g, 0.42 mmol), 2,4-dimethyl-3-ethylpyrrole (112 μL, 0.83 mmol), and a solution of HCl in methanol (1.25 M, 0.66 mL). Compound **1b**·HCl (0.130 g, 82 %) was obtained as a dark-purple solid. ^{1}H NMR (300 MHz, $CDCl_3$): δ = 12.93 (s, 1H; NH), 12.83 (s, 1H; NH), 12.26 (s, 1H; NH), 7.58 (d, J = 7.5 Hz, 1H; ArH), 7.56 (d, J = 7.5 Hz, 1H; ArH), 7.28 (t, J = 7.5 Hz, 1H; ArH), 7.09 (t, J = 7.5 Hz, 1H; ArH), 7.08 (s, 1H), 7.06 (s, 1H), 6.28 (s, 1H), 4.00 (s, 3H; OCH_3), 2.60 (s, 3H; CH_3), 2.41 (q, J = 7.8 Hz, 2H; CH_2) 2.23 (s, 3H; CH_3), 1.08 ppm (t, J = 7.8 Hz, 3H; CH_3); ^{13}C NMR (75 MHz, $CDCl_3$): δ = 164.39, 150.27, 145.18, 139.43, 138.74, 129.44, 127.86, 127.35, 125.29, 125.20 (CH), 121.19 (CH), 120.66 (CH), 119.29, 114.39 (CH), 112.60 (CH), 108.05 (CH), 93.88 (CH), 58.59

© 2011 Wiley-VCH Verlag GmbH & Co. KGaA, Weinheim

(OCH_3), 17.21 (CH_2), 14.57 (CH_3), 12.51 (CH_3), 9.88 ppm (CH_3); HRMS (EI): *m/z* calcd for $C_{22}H_{23}N_3O$: 345.1841; found: 345.1823.

Compound 1c·HCl: Compound **1c**·HCl was prepared as described for **1a**·HCl from **6** (0.1 g, 0.42 mmol), 4,5,6,7-tetrahydroindole (0.101 g, 0.83 mmol), and a solution of HCl in methanol (1.25 M, 0.66 mL). Compound **1c**·HCl (0.035 g, 22%) was obtained as a dark-purple solid. ^{1}H NMR (300 MHz, $CDCl_3$): δ = 13.09 (s, 1H; NH), 12.95 (s, 1H; NH), 7.60 (d, J = 8.7 Hz, 2H; ArH), 7.31 (t, J = 6.9 Hz, 1H; ArH), 7.15 (d, J = 2.1 Hz, 1H; ArH), 7.11 (t, J = 7.2 Hz, 1H; ArH), 7.06 (s, 1H), 6.71 (s, 1H), 6.29 (d, J = 2.1 Hz, 1H), 4.02 (s, 3H; OCH_3), 3.04 (t, J = 6.0 Hz, 2H; CH_2) 2.56 (t, J = 6.0 Hz, 3H; CH_2), 1.82 ppm (m, 4H; 2×CH_2); ^{13}C NMR (75 MHz, $CDCl_3$): δ = 165.23, 152.04, 146.89, 139.08, 128.51 (CH), 127.86, 127.03, 126.75, 126.03, 125.75 (CH), 121.40 (CH), 120.90 (CH), 120.66, 117.97 (CH), 112.81 (CH), 109.16 (CH), 94.09 (CH), 58.77 (OCH_3), 24.17 (CH_2), 22.92 (CH_2), 22.57 (CH_2), 22.12 ppm (CH_2); HRMS (EI): *m/z* calcd for $C_{22}H_{21}N_3O$: 343.17; found: 343.46.

Compound 2·HCl: Under an inert atmosphere, **6** (0.03 g, 0.12 mmol) was dissolved in methanol (1.5 mL) and a solution of HCl in methanol (1.25 M, 0.20 mL) was added dropwise. The color changed to dark blue and the mixture was stirred for 48 h. The solid formed was filtered off and washed with cold methanol (1 mL) to afford compound **2**·HCl (0.028 g, 95%) as a deep-blue solid. ^{1}H NMR (300 MHz, [D_6]DMSO): δ = 12.82 (s, 2H; NH), 12.02 (s, 2H; NH), 7.79 (s, 1H), 7.68 (d, J = 8.1 Hz, 1H; ArH), 7.49 (d, J = 8.4 Hz, 1H; ArH), 7.28 (t, J = 8.1 Hz, 1H; ArH), 7.13 (s, 1H), 7.12 (t, J = 7.5 Hz, 1H; ArH), 6.88 (s, 1H), 4.03 ppm (s, 3H; OCH_3); ^{13}C NMR (75 MHz, [D_6]DMSO): δ = 163.71, 143.38, 138.17, 127.97, 127.73, 124.83, 121.53 (CH), 120.67 (CH), 118.24 (CH), 111.78 (CH), 109.73 (CH), 107.22 (CH), 95.17 (CH), 59.05 ppm (CH_3); HRMS (EI): *m/z* calcd for $C_{27}H_{22}N_4O_2$: 434.1743; found: 434.1755.

Compound 3·HCl: Under an inert atmosphere, **5** (0.1 g, 0.29 mmol) was dissolved in methanol (5 mL). 2,4-Dimethylpyrrole (51 μL, 0.50 mmol) was added, followed by dropwise addition of a solution of HCl in methanol (1.25 M, 0.40 mL). The color changed to dark red and the mixture was stirred for 2 h. The solvent was removed and the solid obtained was washed with acetone (3 mL) and filtered to afford **3**·HCl (0.103 g, 77%) as a dark-purple solid. ^{1}H NMR (300 MHz, $CDCl_3$): δ = 12.90 (s, 1H; NH), 12.34 (s, 1H; NH), 8.11 (d, J = 7.8 Hz, 1H; ArH), 7.70 (s, 1H), 7.66 (d, J = 7.8 Hz, 1H; ArH), 7.38 (t, J = 7.8 Hz, 1H; ArH), 7.26 (t, J = 7.8 Hz, 1H; ArH), 6.13 (s, 1H), 6.04 (s, 1H), 4.00 (s, 3H; OCH_3), 2.62 (s, 3H; CH_3), 2.34 (s, 3H; CH_3), 1.59 ppm (s, 9H; $(CH_3)_3$); ^{13}C NMR (75 MHz, [D_6]DMSO): δ = 164.60, 153.65, 148.73, 146.03, 145.73, 137.89, 128.64, 128.03, 126.96 (CH), 126.35, 123.84 (CH), 122.07 (CH), 118.75, 117.47 (CH), 117.17 (CH), 116.06 (CH), 115.19 (CH), 98.32 (CH), 84.75, 59.48 (OCH_3), 27.38 ($(CH_3)_3$), 13.99 (CH_3), 11.72 ppm (CH_3); HRMS (EI): *m/z* calcd for $C_{25}H_{27}N_3O_3$: 417.2052; found: 417.2054.

Compound 4: Compound **1a**·HCl (0.05 g, 0.14 mmol) was dissolved in CH_2Cl_2 (8 mL) and placed in an ice bath. Et_3N (145 μL, 1.04 mmol) was added dropwise. After 5 min, BF_3·OEt_2 (153 μL, 1.04 mmol) was added dropwise. The mixture was stirred for 48 h at RT. The organic solution was washed with water and the organic residue chromatographed (SiO_2, CH_2Cl_2) to afford **4** (32 mg, 62%) as a purple solid. R_f = 0.9 (CH_2Cl_2); ^{1}H NMR (300 MHz, $CDCl_3$): δ = 10.20 (s, 1H; NH), 7.62 (d, J = 8.1 Hz, 1H; ArH), 7.50 (d, J = 8.1 Hz, 1H; ArH), 7.28 (t, J = 8.1 Hz, 1H; ArH), 7.17 (s, 1H), 7.13 (s, 1H), 7.12 (t, J = 8.1 Hz, 1H; ArH), 6.32 (s, 1H), 6.08 (s, 1H), 3.97 (s, 3H; OCH_3), 2.59 (s, 3H; CH_3), 2.25 ppm (s, 3H; CH_3); ^{13}C NMR (75 MHz, $CDCl_3$): δ = 162.40, 153.66, 147.53, 138.79, 138.24, 132.07, 129.08, 127.82, 126.61, 124.61 (CH), 121.15 (CH), 120.57 (CH), 118.42 (CH), 116.45 (CH), 112.13 (CH), 108.48 (CH), 97.97 (CH), 58.39 (OCH_3), 14.72 (CH_3), 11.21 ppm (CH_3); HRMS (EI): *m/z* calcd for $C_{20}H_{18}BF_2N_3O$: 365.1511; found: 365.1522.

Single-crystal X-ray diffraction analysis: Single crystals of **1a**·HCl, **3**·HCl, and **4** were coated in high-vacuum grease and mounted on a glass fiber. X-ray measurements were made with a Bruker SMART CCD area-detector diffractometer with $Mo_{K\alpha}$ radiation (λ = 0.71073 Å), beam size 0.5 mm. Intensities were integrated from several series of exposures, each covering 0.3° in ω, a hemisphere of data were recorded. For **1a**·$MeSO_3H$ data were collected on a Bruker Nonius KappaCCD APEXII diffractometer mounted at the window of a Molybdenum rotating anode (λ-($Mo_{K\alpha}$) = 0.71073 Å). ϕ and ω scans were carried out to fill the asymmetric unit. Data collection and processing were carried out by using the programs COLLECT[18] and DENZO.[19] Absorption corrections for all samples were applied, based on multiple and symmetry-equivalent measurements by using the program SADABS.[20,21] The structures were solved by direct methods and refined by least squares on weighted F2 values for all reflections.[22] All non-hydrogen atoms were assigned anisotropic displacement parameters and refined without positional constraints. All hydrogen atoms were constrained to ideal geometries and refined with fixed isotropic-displacement parameters. Refinement proceeded smoothly to give the residuals shown in Table 3. Complex neutral-atom scattering factors were used.[23] For **3**, thermal parameters and geometrical restraints were applied to the disordered solvent. Hydrogen atoms of the NH groups were freely refined. CCDC-825757 (**1a**·HCl), CCDC-825755 (**1a**·MeSO3H), CCDC-825758 (**3**·HCl), and CCDC-825756 (**4**) contains the supplementary crystallographic data for this paper. These data can be obtained free of charge from The Cambridge Crystallographic Data Centre via www.ccdc.cam.ac.uk/data_request/cif.

Computational methods: The geometries of the complexes studied in this report were optimized without any symmetry constraints. In these calculations we used the BP86 density functional[24,25] in conjunction with the Ahlrichs quadruple-ζ plus polarization (def2-QZVP) basis sets[26] for all atoms. The reported BP86 calculations were carried out at the resolution of the identity (RI) level. Therefore, we have used the parallel RI-DFT methodology,[27,28] which uses an auxiliary fitting basis[29] to avoid treating the complete set of two-electron repulsion integrals, thus speeding up the

Table 3. Selected crystal-structure data for **1a**·HCl, **1a·MeSO$_3$H**, **3**, and **4**.

Compound	**1a**·HCl	**1a**·$MeSO_3H$	**3**·HCl	**4**
Chemical formula	$C_{20.5}H_{21}Cl_2N_3O$	$C_{21}H_{23}N_3O_4S$	$C_{25}H_{28}N_3O_3$·0.25($C_4H_{10}O$).Cl	$C_{20}H_{18}BF_2N_3O$
Formula mass	396.30	413.48	472.48	365.18
Crystal size [mm]	0.50×0.10×0.10	0.10×0.04×0.01	0.55×0.40×0.20	0.20×0.10×0.10
Crystal system	Monoclinic	Monoclinic	Monoclinic	Monoclinic
a [Å^{-1}]	25.684(4)	12.3961(8)	29.642(9)	12.591 (3)
b [Å^{-1}]	7.9002(13)	7.7364(4)	11.438(3)	8.2840 (19)
c [Å^{-1}]	23.340(4)	20.6776(13)	15.641(5)	16.546 (4)
β [°]	121.753(3)	95.977(3)	90.273(6)	96.960 (4)°
Unit cell volume [Å^3]	121.753(3)	1972.2(2)	5303(3)	1713.1 (7)
T [K]	298	120(2)	298	298
Space group	*C2/c*	*P21/n*	*C2/c*	*P2$_1$/c*
Z	8	4	8	4
No. of reflections measured	19156	18440	25594	15956
No. of independent reflections	3550	3461	4667	2994
R_{int}	0.232	0.1518	0.071	0.0664
Final R_1 values ($I>2\sigma(I)$)	0.0892	0.1347	0.0748	0.0458
Final $wR(F^2)$ values ($I>2\sigma(I)$)	0.2107	0.2175	0.2064	0.1241
Final R_1 values (all data)	0.1458	0.2243	0.1147	0.0557
Final $wR(F^2)$ values (all data)	0.2455	0.2570	0.2374	0.1441

© 2011 Wiley-VCH Verlag GmbH & Co. KGaA, Weinheim

calculations significantly. We computed the interaction energy for each complex by subtracting the total energy of the optimized reference monomers from the total energy of the complex in the optimized geometry. The environment effects (with water as solvent) were taken into account by the COSMO[30] continuum solvation model. For all compounds we have carried out geometry optimization in water at the RI-BP86/def2-QZVP level. All calculations were performed using the TURBOMOLE program, version 6.1.[31]

Cell culture materials and methods: Human SCLC cell line GLC4 were cultured in RPMI 1640 medium (Biological Industries, Beit Haemek, Israel), supplemented with10% fetal bovine serum (FBS), penicillin (100 U mL^{-1}), streptomycin (100 μg mL^{-1})—all from GIBCO BRL, Paisley, UK—and L-glutamine (2 mM, Sigma Chemicals Co, St Louis, MO, USA) at 37 °C under 5% CO_2 in air.

Vital fluorescence microscopy: The living cultured cells were stained with acridine orange (AO).[32] Briefly, cells on a chamber slide were incubated in the presence (800 nM) and absence of **1--4** in RPMI supplemented with 10% FBS at 37 °C for 15 min–1 h. After three washes with phosphate buffered saline (PBS), the cells were incubated with AO (5 μg mL^{-1}) in PBS for 30 min. The chamber slides were washed with PBS solution supplemented with 10% FBS (×3) and then examined with a Nikon microscope (E800) and photographed with a Diagnostic Instruments photo automat system (Spot JR).

Cell viability assay: Cell viability was determined by the MTT assay.[33] Briefly, 20×10^3 cells were incubated in 96-well microtiter cell-culture plates, in the absence (control cells) or presence (100–800 nM) of **1**–**4** in a final volume of 100 μL. After 24, 48, and 72 h incubation, a solution of MTT in PBS (10 mM) of was added to each well for an additional 4 h. The blue MTT formazan precipitate was dissolved in 24:1 isopropanol/1 N HCl (100μl) and the absorbance at 570 nm was measured on a multiwell plate reader. Cell viability was expressed as a percentage of control. Data are shown as the mean value (standard error of the mean (SEM), $n=6$) of triplicate cultures.

Acknowledgements

The authors thank Consejería de Educación de la Junta de Castilla y León (project BU005B09) and the MICINN of Spain (project CTQ2009–12631-BQU and projectCTQ2008–00841/BQU, FEDER funds) for financial support. This work has been partially supported by a grant from the Spanish government (FIS) and the European Union (PI10/00338, R.P.T.). We thank CONSOLIDER-Ingenio2010 (CSD2010–0065) and the CESCA for computational facilities. D.Q. and R.Q. thank the MICINN of Spain for a "Ramón y Cajal" contract. We also thank Marta Mansilla and Dr. Jacinto Delgado (SCAI-Universidad de Burgos) for the X-ray structure of compound **4**. We thank the reviewers for helpful comments.

[1] For reviews see: a) A. P. Davis, D. N. Sheppard, B. D. Smith, *Chem. Soc. Rev.* **2007**, *36*, 348; b) J. T. Davis, O. A. Okunola, R. Quesada, *Chem. Soc. Rev.* **2010**, *39*, 3843; c) P. A. Gale, *Acc. Chem. Res.* **2011**, *44*, 216; d) G. W. Gokel, N. Barkey, *New J. Chem.* **2009**, *33*, 947. For recent examples, see: e) R. E. Dawson, A. Hennig, D. P. Weimann, D. Emery, V. Ravikumar, J. Montenegro, T. Takeuchi, S. Gabutti, M. Mayor, J. Mareda, C. A. Schalley, S. Matile, *Nature Chem.* **2010**, *2*, 533; f) A. Hennig, L. Fischer, G. Guichard, S. Matile, *J. Am. Chem. Soc.* **2009**, *131*, 16889; g) J. Mareda, S. Matile, *Chem. Eur. J.* **2009**, *15*, 28; h) S. Hussain, P. R. Brotherhood, L. W. Judd, A. P. Davis, *J. Am. Chem. Soc.* **2011**, *133*, 1614.

[2] a) R. Pajewski, R. Garcia-Medina, S. L. Brody, W. M. Leevy, P. H. Schlesinger, G. W. Gokel, *Chem. Commun.* **2006**, 329; b) X. Li, B. Shen, X.-Q. Yao, D. Yang, *J. Am. Chem. Soc.* **2007**, *129*, 7264; c) X. Li, B. Shen, X.-Q. Yao, D. Yang, *J. Am. Chem. Soc.* **2009**, *131*, 13676; d) P. Iglesias Hernández, D. Moreno, A. Araujo Javier, T. Torroba, R. Pérez-Tomás, R. Quesada, *Chem. Commun.* **2012**, DOI: 10.1039/C1CC11300C.

[3] J. T. Davis, *Top. Heterocycl. Chem.* **2010**, *24*, 145.

[4] A. Fürstner, *Angew. Chem.* **2003**, *115*, 320; *Angew. Chem. Int. Ed.* **2003**, *42*, 308.

[5] a) N. R. Williamson, P. C. Fineran, F. J. Leeper, G. P. C. Salmond, *Nature Rev. Microbiol.* **2006**, *4*, 887; b) N. R. Williamson, P. C. Fineran, T. Gristwood, S. R. Chawrai, F. J. Leeper, G. P. C. Salmond, *Future Microbiol.* **2007**, *2*, 605; c) M. S. Melvin, M. W. Calcutt, R. E. Noftle, R. A. Manderville, *Chem. Res. Toxicol.* **2002**, *15*, 742; d) R. Pérez-Tomás, B. Montaner, E. Llagostera, V. Soto-Cerrato, *Biochem. Pharmacol.* **2003**, *66*, 1447.

[6] J. L. Sessler, L. R. Eller, W.-S. Cho, S. Nicolaou, A. Aguilar, J. T. Lee, V. M. Lynch, D. J. Magda, *Angew. Chem.* **2005**, *117*, 6143; *Angew. Chem. Int. Ed.* **2005**, *44*, 5989.

[7] a) R. Pandey, R. Chander, K. B. Sainis, *Curr. Pharm. Des.* **2009**, *15*, 732; b) R. Pérez-Tomás, M. Viñas, *Curr. Med. Chem.* **2010**, *17*, 2222.

[8] M. Nguyen, R. C. Marcellus, A. Roulston, M. Watson, L. Serfass, S. R. M. Madiraju, D. Goulet, J. Viallet, L. Bélec, X. Billot, S. Acoca, E. Purisima, A. Wiegmans, L. Cluse, R. W. Johnstone, P. Beauparlant and G. C. Shore, *Proc. Natl. Acad. Sci. USA* **2007**, *104*, 19512.

[9] a) M. Konopleva, J. Watt, R. Contractor, T. Tsao, D. Harris, Z. Estrov, W. Bornmann, H. Kantarjian, J. Viallet, I. Samudio, M. Andreeff, *Cancer Res.* **2008**, *68*, 3413; b) R. L. Smoot, B. R. A. Blechacz, N. W. Werneburg, S. F. Bronk, F. A. Sinicrope, A. E. Sirica, G. J. Gores, *Cancer Res.* **2010**, *70*, 1960.

[10] K. Daïri, Y. Yao, M. Faley, S. Tripathy, E. Rioux, X. Billot, D. Rabouin, G. Gonzalez, J.-F. Lavallée, G. Attardo, *Org. Process Res. Dev.* **2007**, *11*, 1051.

[11] H. H. Wasserman, D. J. Friedland, D. A. Morrison, *Tetrahedron Lett.* **1968**, *9*, 641.

[12] M. J. Hynes, *J. Chem. Soc. Dalton Trans.* **1993**, 311.

[13] K. Chen, N. S. Rannulu, Y. Cai, P. Lane, A. L. Liebl, B. B. Rees, C. Corre, G. L. Challis, R. B. Cole, *J. Am. Soc. Mass Spectrom.* **2008**, *19*, 1856–1866.

[14] a) B. A. McNally, A. V. Koulov, T. N. Lambert, B. D. Smith, J.-B. Joos, A. L. Sisson, J. P. Clare, V. Sgarlata, L. W. Judd, G. Magro, A. P. Davis, *Chem. Eur. J.* **2008**, *14*, 9599; b) P. A. Gale, C. Tong, C. J. E. Haynes, O. Adeosun, D. E. Gross, E. Karnas, E. M. Sedenberg, R. Quesada, J. L. Sessler, *J. Am. Chem. Soc.* **2010**, *132*, 3240.

[15] S. Bhosale, S. Matile, *Chirality* **2006**, *18*, 849.

[16] a) J. T. Davis, P. A. Gale, O. A. Okunola, P. Prados, J. C. Iglesias-Sanchez, T. Torroba, R. Quesada, *Nature Chem.* **2009**, *1*, 138; b) N. Busschaert, P. A. Gale, C. J. E. Haynes, M. E. Light, S. J. Moore, C. C. Tong, J. T. Davis, W. A. Harrell Jr., *Chem. Commun.* **2010**, *46*, 6252; c) N. J. Andrews, C. J. E. Haynes, M. E. Light, S. J. Moore, C. C. Tong, J. T. Davis, W. A. Harrell, Jr., P. A. Gale, *Chem. Sci.* **2011**, *2*, 256.

[17] A. C. Allison, M. R. Young in *Lysosomes in Biology and Pathology, Vol. 2* (Eds: J. T. Dingle, H. B. Fell), Amsterdam, North Holland, **1969**, pp. 600–628.

[18] COLLECT data collection software, Nonius B. V., **1998**.

[19] Z. Otwinowski, W. Minor in *Methods in Enzymology, Vol. 276: Macromolecular Crystallography, part A* (Eds.: C. W. Carter, Jr., R. M. Sweet), Academic Press, New York, **1997**, p. 307–326.

[20] SADABS 2007/2 (Sheldrick, G. M., 2007).

[21] G. M. Sheldrick. SADABS: A program for absorption correction with the Siemens SMART system; University of Göttingen: Germany, **2001**.

[22] SHELXTL program system version 6.1; Bruker Analytical X-ray Instruments Inc., Madison, WI, **1998**.

[23] *International Tables for Crystallography, Vol. C* (Ed.: A. J. C. Wilson), Kluwer, Dordrecht, **1992**.

[24] A. D. Becke, *Phys. Rev. A* **1988**, *38*, 3098.

[25] J. P. Perdew, *Phys. Rev. B* **1986**, *33*, 8822.

[26] F. Weigend, R. Ahlrichs, *Phys. Chem. Chem. Phys.* **2005**, *7*, 3297–3305.

[27] K. Eichkorn, O. Treutler, H. öhm, M. Häser, R. Ahlrichs, *Chem. Phys. Lett.* **1995**, *242*, 652.

[28] M. Von Arnim, R. Ahlrichs, *J. Comput. Chem.* **1998**, *19*, 1746.

 © 2011 Wiley-VCH Verlag GmbH & Co. KGaA, Weinheim

[29] F. Weigend, *Phys. Chem. Chem. Phys.* **2006**, *8*, 1057.
[30] A. Klamt, G. Schüürmann, *Chem. Soc. Perkin Trans. 2* **1993**, 799.
[31] TURBOMOLE V6.1 2009, a development of University of Karlsruhe and Forschungszentrum Karlsruhe GmbH, 1989–2007, TURBOMOLE GmbH, since 2007; available from http://www.turbomole.com.
[32] E. Holtzman, *Lysosomes*, Plenum Press, New York, **1989**, pp. 95–100.
[33] T. Mosmann, *J. Inmunol. Methods* **1983**, *65*, 55–63.

Received: May 19, 2011
Published online: November 9, 2011

 © 2011 Wiley-VCH Verlag GmbH & Co. KGaA, Weinheim